PUSHOVER ANALYSIS OF CONFINED MASONRY WALLS USING EQUIVALENT DIAGONAL STRUT MODELS

Nemanja Krtinić [(1)], Matija Gams [(2)], Marko Marinković [(3)]

[(1)] *Young researcher, Faculty of Civil and Geodetic Engineering, University of Ljubljana, nkrtinic@fgg.uni-lj.si*
[(2)] *Assistant professor, Faculty of Civil and Geodetic Engineering, University of Ljubljana, mgams@fgg.uni-lj.si*
[(3)] *Assistant professor, Faculty of Civil Engineering, University of Belgrade, mmarinkovic@grf.bg.ac.rs*

Abstract

Masonry structures are commonly used for building residential buildings throughout the Balkans and worldwide, in urban and rural areas and areas with seismic risk. For masonry construction in regions with seismic risk, confined masonry (CM) construction offers an appealing alternative to unreinforced masonry (URM) due to its better seismic performance. The numerical simulation of CM is often based on the Equivalent Strut Model (ESM). Such a model provides a very reasonable compromise between accuracy and efficiency and is simple enough for use in design. The purpose of this paper is to compare the results of an experimental shear compression test on a modern CM wall with different ESM models. Five ESM models proposed by various authors are compared. The numerical pushover analyses were performed in the SAP2000 software, and the reference points of the model that gave the best alignment with experimental results were estimated using regression analyses. The results show that the simple modelling of CM walls with an equivalent diagonal strut, which carries load only in compression, can accurately simulate the global seismic response and is suitable for practical applications.

Keywords: Confined masonry, Equivalent strut model (ESM), Numerical modelling, Pushover analysis, SAP2000.

1. Introduction

Masonry structures are traditionally used for low- to mid-rise buildings, particularly in regions characterised by high seismic hazard. Although unreinforced masonry structures did not perform well during the past earthquakes in Italy, the Balkans (Croatia, Slovenia, Serbia and Albania), Latin America (Chile, Peru and Mexico), the Middle East and South Asia, masonry is still one of the most commonly used building materials in earthquake-prone areas. Field observations after major earthquakes showed that earthquakes could cause significant damage to structures or even total collapse. Therefore, many researchers are working to prevent or reduce the consequences of earthquakes with alternative construction technologies with improved seismic performance.

One such technology is confined masonry, consisting of masonry walls and reinforced concrete (RC) confining elements. The confining tie-columns and tie-beams fully enclose the walls in vertical and horizontal directions [1]. These RC ties effectively improve the integrity and stability of masonry walls to in-plane and out-of-plane earthquake effects [2]. In the past decades, CM buildings have withstood major earthquakes, such as the 2010 Chile earthquake, which caused substantial damage to URM masonry and RC buildings without collapse [3]. It should also be noted that properly constructed confined masonry buildings performed very well and substantially better than URM buildings in the recent Petrinja, Croatia M 6.4 earthquake [4].

Confined masonry technology presents a viable alternative for unreinforced masonry (URM) and reinforced concrete (RC) frames with masonry infills because it does not require advanced construction skills and equipment. The increasing use of confined masonry requires reliable methods for structural response analysis, not only for the design of new construction but also for evaluating existing buildings [5].

Most research on CM is based on experimental testing of walls subjected to in-plane lateral loading [6, 7]. In contrast, there appears to be less research on the numerical modelling of CM walls. However, it is essential both for research and design to supplement and extend experimental results and to derive

appropriate computational models. Marques et al. [8] discussed several numerical models currently available for the seismic analysis of CM structures. Confined masonry walls exhibit complex and highly inelastic behaviour during seismic loading. Therefore, their proper consideration requires sophisticated computational techniques, which are usually not practical for designers. The finite element method-based approaches differ in degrees of refinement and accuracy. They can generally be divided into three groups: detailed micro model, simplified micro model and macro model. An appropriate approach is chosen depending on the analysis's purpose and the required detail level.

The numerical simulation of CM is often based on a macro-modelling approach, i.e. Equivalent Strut Model (ESM). This most straightforward type of modelling requires less computational effort and is suitable for routine design, wherein a compromise between accuracy and efficiency is needed [9]. The aim of this paper is to compare five nonlinear ESM models proposed by different authors with the experimentally obtained response of modern CM walls. The experimental tests were in-plane cyclic shear compression tests.

The following section presents the Equivalent Strut Models used in the analyses, with an additional theoretical explanation. The experimental investigation of two modern CM walls, as well as the results of the experiment, are briefly described in section 3. The numerical model was built in the SAP 2000 software [19]. Model calibrations and a comparison between experimental and numerical results are presented in section 4, followed by conclusions.

2. The Equivalent Strut Models (ESMs)

The Equivalent Strut Model (ESM) is one of the most known macro models, which was first proposed in the 1960s to model masonry infills in RC frames with diagonal struts. The diagonal strut model arose from the observation that during horizontal in-plane loading of an RC frame with masonry infill, the compression field in the masonry infill develops mainly along its diagonal (see Fig. 1b). Several researchers have later proposed using the ESM to model CM structures [10]. The present work was guided by the assumption that failure modes in CM walls and RC frames with infills are similar.

In case the ESM model is used in a linear analysis for, e.g. design, the only required parameters are the modulus of elasticity and the strut dimensions. For nonlinear analysis, on the other hand, the whole axial force-displacement curve is needed [11]. In the past decades, many researchers [12-16] have proposed approaches to model the lateral force-displacement relationship. These can represent the masonry wall's monotonic or cyclic behaviour, both of which are calculated based on the mechanical and geometrical characteristics explained below.

A multilinear relationship usually describes the constitutive law of an equivalent strut. Various models [13, 16, 17] have been proposed that take into account multiple failure modes and, based on the expected failure mode, calculate the lateral strength of the panel. However, other proposed models [12, 14, 15] seem to be easier to apply because they only require knowledge of the mechanical properties of the wall, even if they do not predict failure modes. It should be noted that in the proposed models, the initial stiffness and strength refer to the horizontal direction and have to be transformed to the diagonal (strut) direction. The models used in this study and corresponding equations to determine the envelope of the force-displacement curve for the lateral strength F or the strut axial strength N are shown in Table 1.

If the strut axial strength N is determined first, the lateral strength of the wall F is obtained using the following equation:

$$F = N \cos\varphi \qquad (12)$$

The model by Panagiotakos and Fardis [12] used a four-linear lateral force-displacement curve that describes the cracking force, peak strength and residual strength after the failure of the masonry infill, as shown in Fig. 2a. The maximum lateral strength (F_m in Fig. 2a) is assumed equal to 1.3 times the cracking strength, while the lateral residual strength (F_u in Fig. 2a) is taken as 10% of the peak strength. The ultimate strength of the wall is a function of the masonry shear strength determined from the diagonal compression test τ_{cr} (Eq. (1)).

Table 1 – Equations for the strut axial strength or lateral strength

Reference	Lateral strength F / Strut axial strength N	
Panagiotakos and Fardis [12]	$F_{max} = 1.3 f_{ms} l_m t_m$	(1)
Decanini et al. [13]	$N_{dt} = \left(0.6\tau_{m0} + 0.3\sigma_0\right) t_w d$	(2)
	$N_s = \left(\left(1.2\sin\theta + 0.45\cos\theta\right)\tau_0 + 0.3\sigma_0\right) t_w d$	(3)
	$N_{cc} = \dfrac{1.12\sin\theta\cos\theta}{K_1\left(\lambda_h\right)^{-0.12} + K_2\left(\lambda_h\right)^{0.88}}\sigma_{m0} t_w d$	(4)
	$N_{dc} = \dfrac{1.16\sigma_{m0}\tan\theta}{K_1 + K_2\lambda_h} t_w d$	(5)
Dolšek and Fajfar [14]	$F_m = 0.818\dfrac{L_{in} t_w f_{tp}}{C_I}\left(1 + \sqrt{C_I^{\,2}+1}\right)$	(6)
Teni et al. [15]	$F_{max} = 1.3\tau_{cr} l_w t_w$	(7)
Liberatore et al. [16]	$N_s = \left(\left(1.2\sin\varphi + 0.45\cos\varphi\right)\tau_0 + 0.3\sigma_y\right) t d$	(8)
	$N_{dt} = \left(0.6\tau_{m0} + 0.3\sigma_y\right) t l_m$	(9)
	$N_{dc} = 1.16\tan\varphi\, f_m\,\lambda_h^{-1}$	(10)
	$N_{cc} = 1.12\sin\varphi\cos\varphi\, f_m\,\lambda_h^{-0.88}$	(11)

F_{max} - maximum strength of masonry wall; N_{dt} - strength in the diagonal tension failure mode; N_s - strength in the bed-joint sliding failure mode; N_{cc} - strength in the corner compression failure mode; N_{dc} - strength in the diagonal compression failure mode; $l_w, d, L_{in}, l_m, \theta, \varphi$ - geometrical characteristics (see Fig. 1); t_w, t_m, t – wall thickness; $\tau_{cr}, \tau_{m0}, f_{ms}$ - shear strength evaluated through diagonal compression tests; τ_0 - shear strength of bed joints; f_{tp} - referential tensile strength of masonry; f_m, σ_{m0} - compression strength of masonry; σ_0, σ_y - vertical stress of the applied load; C_I - coefficient of interaction between the wall and the surrounding frame; λ_h - non-dimensional parameter (Eq. (18)); K_1, K_2 - empirical coefficients (see Table 2).
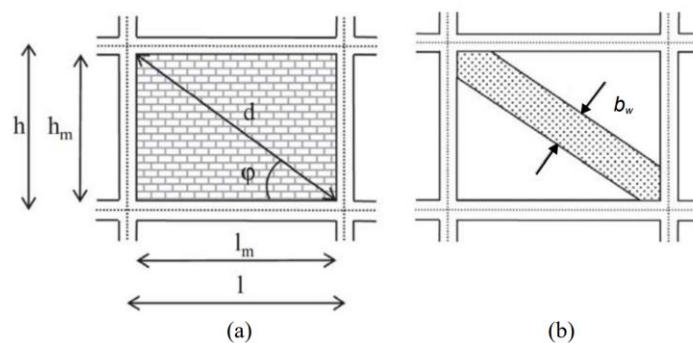

Figure 1. Equivalent strut model: (a) in-plane geometrical characteristics and (b) equivalent diagonal strut [16].

The most physically sound approach considers all possible failure mechanisms in masonry. Therefore, it is necessary to calculate the strength associated with each mechanism and then adopt the lowest value, which is the most likely failure mode that can occur when the wall is loaded. That value is then the assumed strength of the equivalent diagonal strut. The model by Decanini et al. [13] adopted a four-branched backbone curve that describes: (a) the linear elastic uncracked phase H_{mf}; (b) the post-cracking stage until reaching the maximum strength H_{mfc}; (c) the descending branch until H_{mr} and (d) the residual strength characterised by a horizontal line as shown in Fig. 2b. Decanini et al. [13] consider four

different possible failure mechanisms shown in Table 1 (Eqs. (2) – (5)). The strength values related to diagonal tension, N_{dt}, and to sliding shear failure, N_s, depend on the masonry shear strength and the vertical stress acting on the infill. The resistance associated with corner compression, N_{cc}, and diagonal compression, N_{dc}, are a function of the masonry compressive strength.
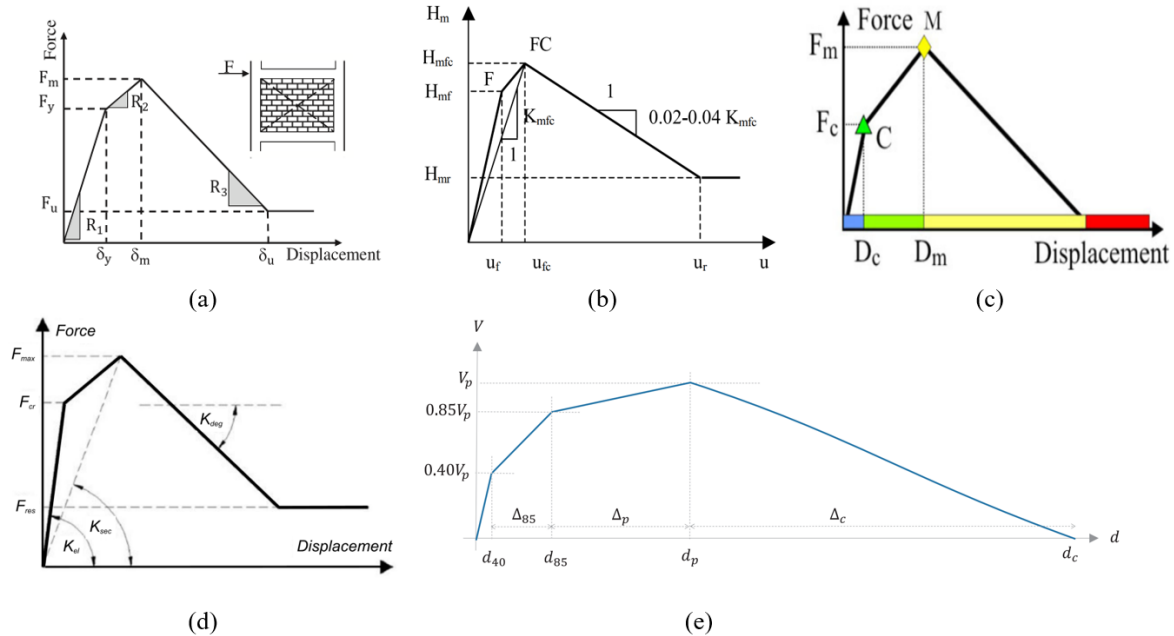

Figure 2. The multilinear force-displacement curve of (a) model by Panagiotakos and Fardis [12]; (b) model by Decanini et al. [13]; (c) model by Dolšek and Fajfar [14]; (d) model by Teni et al. [15] and (e) model by Liberatore et al. [16].

The envelope of the force-displacement curve adopted in the model of Dolšek and Fajfar [14] is presented by three branches (see Fig. 2c). To calculate the maximum strength of the wall F_{max} (Eq. (6)), the expression proposed by Žarnić and Gostič [18] was used. The cracking force F_c is obtained assuming the ratio of F_c/F_{max} of 0.6.

Teni et al. [15] proposed the model shown in Fig. 2d. The behaviour of the diagonal strut is defined with an envelope of horizontal force and displacement, which is adopted from Panagiotakos and Fardis [12]. The difference is that the residual strength (F_{res} in Fig. 2d)) is taken as 30% of F_{max}.

Finally, Liberatore et al. [16] proposed a model that considers uncertainties in its "backbone" curve. The proposed force-displacement curve is defined by four characteristic points (Fig. 2e) with different shear values: 40% of V_p, 85% of V_p, V_p and zero, where V_p is the peak load. The corresponding displacements are d_{40}, d_{85}, d_p and d_c, respectively. For the estimation of the peak load, V_p, Liberatore et al. [16] consider four failure mechanisms (Eqs. (8) – (11)), the same as in the model of Decanini et al. [13]. The strut axial strength, N, is the minimum value among the different failure mechanisms. In addition to the mechanical characteristics of the masonry, this advanced model also takes into account various characteristics, such as the presence of vertical or horizontal holes in the units, the type of test (monotonic or cyclic), etc.

The axial stiffness of the diagonal strut, K_s, is generally calculated as a function of the strut width, b_w, according to the following equation:

$$K_s = \frac{E_m t_w b_w}{d} \tag{13}$$

where E_m is Young's modulus, t_w is the thickness of the masonry wall, and d is the length of the strut. The secant stiffness associated with the load capacity of the wall (K_{sec} in Fig. 2d), determined from the axial stiffness of the equivalent strut, is given by the following equation:

$$K_{sec} = \frac{E_m t_w b_w}{d} \cos^2 \theta \tag{14}$$

The equations used to determine the equivalent strut width that the authors used in their models are shown in Table 2.

Table 2 – Equivalent strut width predictive equations

Reference	Equivalent strut width b_w		
Panagiotakos and Fardis [12]	$b_w = 0.175 \left(\lambda_h \right)^{-0.4} d$		(15)
Decanini et al. [13]	$b_w = \left(\dfrac{K_1}{\lambda_h} + K_2 \right) d$	for $\lambda_h < 3.14$ $\quad K_1 = 3, K_2 = -0.178$ for $3.14 < \lambda_h < 7.85$ $\quad K_1 = 0.707, K_2 = 0.01$ for $\lambda_h > 7.85$ $\quad K_1 = 0.47, K_2 = 0.04$	(16)
Teni et al. [15]	$b_w = 0.175 \left(\lambda h_c \right)^{-0.4} d$		(17)

b_w - the width of the strut; h_c - the column height; d - the length of the compressive diagonal; λ_h – see below

The formula used to calculate the equivalent strut width (Eq. (15)) in the study by Panagiotakos and Fardis [12] is straightforward. The strut width b_w from Eq. (16) is calculated from the non-dimension parameter λ_h and two constants, K_1 and K_2, calibrated from experimental tests [13]. To calculate the strut width b_w, Teni et al. [15] use a slightly modified formula (15), as shown in Table 2 (Eq. (17)).

The width of the strut is based on the dimensionless parameter λ_h, which takes into account the material and geometric characteristics of the frame-infill system

$$\lambda_h = \sqrt[4]{\frac{E_m t_w \sin 2\theta}{4 E_c I_c h_m}} h \tag{18}$$

Where E_c is the elastic modulus of concrete, I_c is the moment of inertia of columns, h_m is the height of the masonry panel, and θ is the slope of the strut relative to the horizontal axis.

Teni et al. [15] use the parameter λ according to a modified equation that has the following form:

$$\lambda = \sqrt[4]{\frac{E_m t_w \sin 2\theta}{4 E_c I_c h_m}} \tag{19}$$

The formulas listed in Table 1 require knowledge of the mechanical and geometric parameters of the masonry wall. Among others, the parameters needed to determine the maximum lateral strength of the wall are the compressive strength of masonry, f_m, the shear strength evaluated through diagonal compression tests, τ_{m0}, and the shear strength of bed joints, τ_0. When parameters τ_{m0} and τ_0 are not available, Liberatore et al. [16] in their study propose the following equations for determining these parameters:
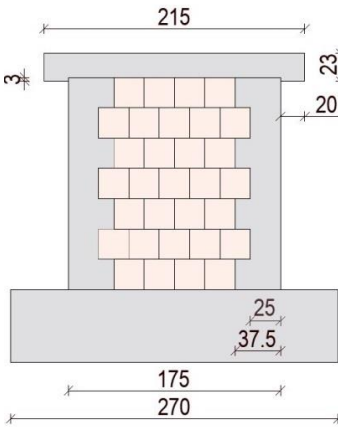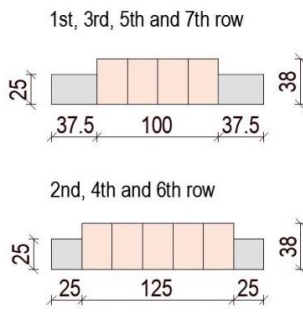
$$\tau_{m0} = 0.285 \sqrt{f_m} \text{ (MPa)} \tag{20}$$

$$\tau_0 = \frac{2}{3} \tau_{m0} = 0.211 \sqrt{f_m} \text{ (MPa)} \tag{21}$$

3. Experimental cyclic shear test

The seismic response of modern CM walls was tested in a cyclic shear compression test on two samples (W7 and W8, see Table 3). In the test, the compressive stress state due to the weight above is modelled by additional vertical forces applied before the lateral load. The seismic load is imposed on the wall in the form of prescribed displacements, which act cyclically in positive and negative directions (three times) and with increasing amplitude until collapse. Finally, the boundary conditions in the test were the so-called fixed-fixed boundary conditions (no rotation at the top with constant vertical force).

Table 3 – Confined masonry walls for cyclic shear tests (dimensions in cm)

The walls were constructed from modern large chamber blocks (nominal dimensions of the unit are 250 x 249 x 380 mm) with insulation material in the chambers and polyurethane (PU) glue instead of mortar. They were built on RC foundations for transport and later fixing to the laboratory floor. There was first a 1–2 cm thick layer of general-purpose mortar on the foundation to provide a level surface for constructing the wall. Wall above was built using PU glue, which was applied to bed joints in four strips. The units were laid into the PU glue, and the final thickness of the bed joint was less than 1 mm. Head joints were unfilled and interlocked with the feather and groove type of contact. Perfect overlapping of units was used (overlap equal to half the length of the unit). RC bond beams were constructed on top of the walls to distribute vertical and horizontal loads during testing. The dimensions of the tested CM walls are shown in Table 3.

3.1 Material properties

Material properties were measured using dedicated tests. Some of the parameters were determined by calculation. Because the diagonal compression test was not performed in the experimental cyclic shear tests of CM walls, the shear cracking strength of masonry τ_{cr} was calculated as 0.285 times the square root of compressive strength of masonry f_m (see Eq. (20)). The shear strength of bed joints, τ_0, was also calculated using Eq. (21). The reference tensile strength of masonry (f_{tp}) can be derived from the diagonal tension test, which was also not performed in this experiment. Žarnić and Gostič [18] predict that this value is usually in the range between 4 % and 8 % of the compressive strength of the wall. In this study, it is assumed that this value was 8 % of f_m.

All relevant parameters are shown in Table 4.

Table 4 – Material property values used for concrete, masonry and reinforcement steel.

Concrete	Value	Source
Elastic modulus of concrete E_c [MPa]	33000	Standard EC2
Masonry		
Elastic modulus of masonry E_m [MPa]	2200	Experiment
Shear strength of masonry τ_{m0} [MPa]	0.556	Calculated
Referential tensile strength of masonry f_{tp} [MPa]	0.304	Calculated
Compressive strength of masonry f_m [MPa]	3.8	Experiment
Basic shear strength of bed joints τ_0 [MPa]	0.411	Calculated
Vertical stress of the applied load σ_0 [MPa]	0.63	Experiment
Reinforcement steel		
Elastic modulus of reinforcement steel E_s [MPa]	200 000	Experiment
Yield tensile strength f_y [MPa]	551	Experiment
Ultimate tensile strength f_u [MPa]	658	Experiment

3.2 Experimental results

The comparison between the numerical pushover analysis and experimental tests is performed on the envelope curves of the response. Fig. 3 shows the envelope curves for both tested walls (W7 and W8) and the average pushover curve used to compare with the results from the numerical simulations.
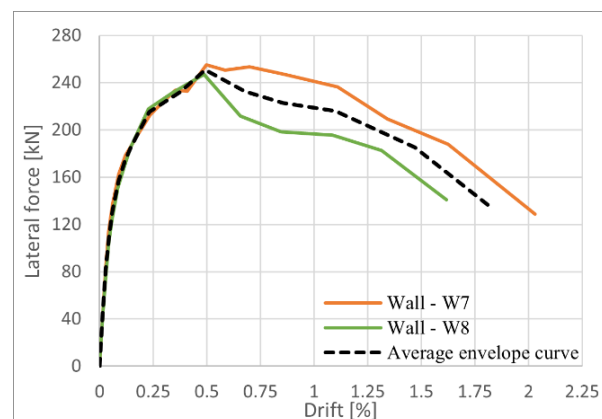

Figure 3. Experimental envelope curves of the tested confined walls.

4. Numerical simulations

4.1 Description of the numerical model

As mentioned in chapter 2, the Equivalent Strut model was used to model the CM wall. The model consists of a frame, which can develop plastic hinges at the corners (Fig. 4a) and a diagonal strut to model the effect of masonry (Fig. 4b). For the frame, interacting P-M2-M3 hinges were used in the tie-columns, and moment M3 hinges were used for the bond beam. Plastic hinges were defined at relative distances of 0.05 and 0.95, as seen in Fig. 4a. The strut is modelled using the "link" elements in SAP2000 [19]. This type of element is used because it can connect two joints (RC ties and wall) and behaves non-linearly. The link element consists of six springs for each of the six degrees of freedom, and different linear or nonlinear properties can be assigned to each spring [19].

The nonlinear characteristics of hinges in the frame were calculated based on the characteristics of the materials taken from experimental tests. Mander's model [20] was used for concrete when defining the

stress-strain curve, which was automatically defined by the program. A stress-strain curve was specified for the rebars based on the mechanical characteristics of the steel (see Table 4).
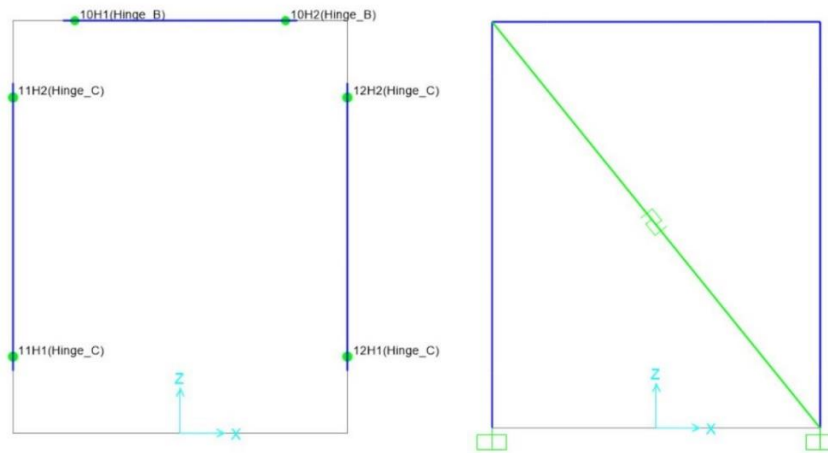

Figure 4. a) Hinge locations in the numerical model [19]; b) Numerical model with diagonal strut [19].

The multilinear plastic "link" element connects two diagonally opposite corners and has defined only the properties in the U_1 direction because the equivalent diagonal strut "works" only in compression. The force-displacement multilinear curve is the nonlinear property assigned to the "link" element. The parameters and formulas that define the force-displacement curves and corresponding constitutive models are shown below.

Fig. 5 shows the final axial force-axial displacement curves for strut proposed by different authors, which serve as input data in numerical analyses.
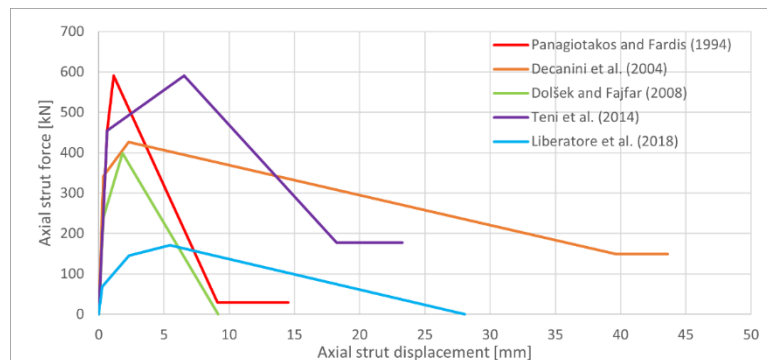

Figure 5. Final axial force-axial displacement curves for strut proposed by various authors.

4.2 Comparison of the results

The results from the numerical pushover analyses were compared to the envelope curve of the test in Fig. 6. The Panagiotakos and Fardis (red) model significantly overestimates peak strength (the relative percentage error e_r=148%). Based on the softening branch of the numerical curve, it can be concluded that these authors' model is more suitable for walls with extremely brittle failure. A similar observation can be made for the Dolšek and Fajfar model (green curve). However, the overestimation of peak strength is smaller, at about 82%.
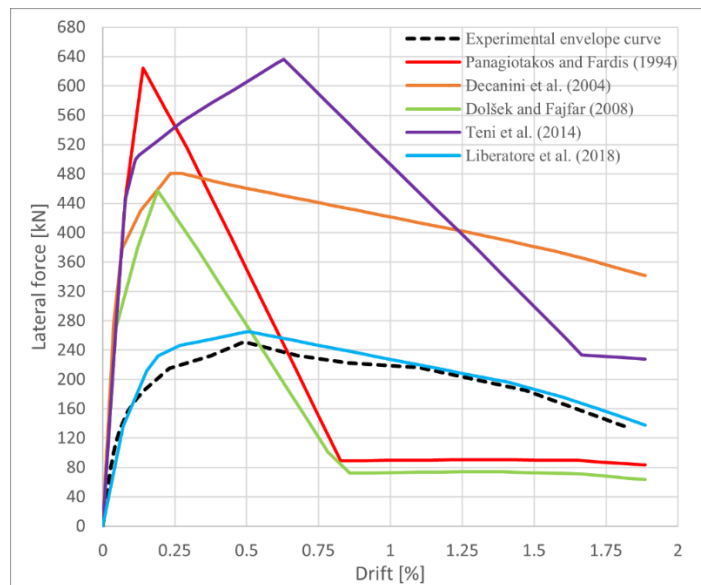
Figure 6. Comparison of the results between the numerical and experimental curves.

The model by Decanini et al. (orange) similarly overestimates peak strength by about 90% and underestimates drift at peak strength. The softening stiffness after reaching peak force is much better estimated, as it aligns with the experiment quite well.

Teni et al. (purple) model significantly overestimates peak strength (153%). However, this model is the only one that overestimates drift at peak resistance (0.63% in the model and 0.49% in the experiment). The model predicts a more brittle response than what was observed in the test.

Finally, the model proposed by Liberatore et al. shows a remarkable resemblance between the numerical model (light blue) and the experimental one (black dashed), as seen in Fig. 6. After the elastic phase, the numerical model curve's peak is reached around 8.9 mm (drift 0.51%). The experimental one peaked at 8.6 mm (drift 0.49%). Moreover, the numerical results match the initial stiffness, peak load capacity and stiffness degradation quite well. Therefore, it can be said that the model proposed by Liberatore et al. [16] is suitable for confined masonry walls of this type.

Relatively bad alignment of models [12-15] with the experiment indicates they should be calibrated to give better results.

4.3 Calibration of models and results

This subsection presents the improved numerical curves of calibrated models [12-15]. The results of the calibrated strut envelopes are shown in Fig. 7.
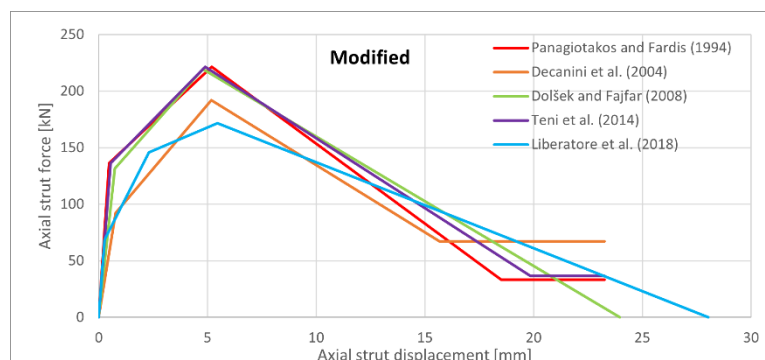

Figure 7. Modified axial force-axial displacement curves for equivalent diagonal strut.

Analysis of experimental values from cracking-to-peak strength (F_{peak}) suggests that such a ratio can be fixed and equal to 0.6 in the models [12] and [15], while the peak strength of the wall is equal to 0.5 τ_{cr} A_w. The residual strength F_{res} is calculated as 15% of the peak strength. The secant stiffness K_{sec} is corrected by factors of 0.2 and 0.5 for models [12] and [15], respectively. Secant-to-cracking stiffness K_{el} and softening stiffness K_{deg} are finally presented as a fraction of K_{sec}. The elastic stiffness was obtained as 3.0 K_{sec} and 2.7 K_{sec} for models [12] and [15], respectively, while the degrading stiffness for both models was adopted as 0.15 K_{sec}.

To better match the experimental results with the numerical results, the model of Dolšek and Fajfar [14] also had to be calibrated. The maximum force F_{max} (see Eq. (6)) was corrected by a factor of 0.55. The cracking force F_c was calculated assuming a ratio between the cracking force and the maximum force of 0.35. Secant stiffness K_{sec} was corrected by a factor of 0.2, while the elastic stiffness K_1 was obtained as 2.0 K_{sec}. It was also concluded that using a modified force-displacement curve for the strut model, the numerical (green) and experimental curves (black dashed) show good similarity, except that the numerical model gives an overestimation of peak strength as in models [12] and [15].

In the calibrated model by Decanini et al. [13], the minimum lateral strength H_{mfc} was considered to be only 45% of the lateral strength previously calculated via the most probable failure mode of the CM wall. The linear elastic uncracked strength H_{mf} is assumed as 50% of lateral strength, while the residual strength H_{mr} takes 35% of H_{mfc}. The stiffness of the wall at the stage of complete cracking K_{mfc} was corrected by a factor of 0.15, which directly affected the uncracked stiffness K_0. A modification for the uncracked stiffness K_0 is also proposed, considering 60% of the calculated elastic stiffness.

Finally, the calibrated model by Decanini et al. shows slightly better results than the previous models in terms of overestimating peak strength (about 12%). The model by Liberatore et al. [16] was not modified because it considered all the uncertainties in its "backbone" curve that the previous four models did not consider.

As in the previous subchapter, all five numerical pushover curves are shown in Fig. 8, and compared with the experimental envelope curve.
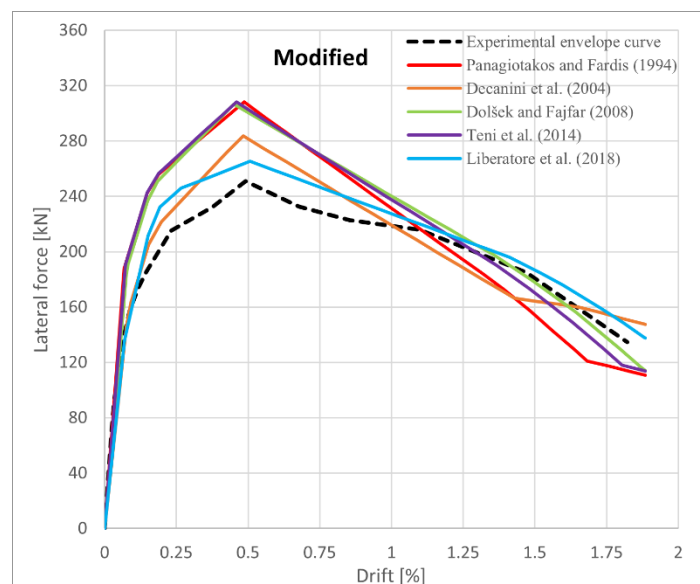

Figure 8. Comparison of the calibrated numerical and experimental curves.

5. Conclusions

Confined masonry (CM) is a construction technology that has the potential for seismically resilient masonry construction. However, the broader application of this technology for the design of new construction and evaluation of existing buildings requires improving relevant codes and developing simple and reliable numerical models for seismic analysis.

The Equivalent Strut Model (ESM) proposed in this study can be used for nonlinear static analysis of CM structures as one of the most straightforward macro-modelling approaches. In this approach, the RC confining elements are modelled as horizontal (beam) and vertical (column) elements, while the masonry wall is modelled as a diagonal strut.

The numerical analyses were performed in the SAP2000 software using five models of force-displacement curves for the confined masonry wall proposed by the various authors. Straightforward use of the models showed significant discrepancies with the experiments, except in the case of Liberatore et al. model. In the next step, the models were calibrated, and the alignment with the experiments was much better. The following conclusions have been drawn based on this study:

- Simple modelling with an equivalent diagonal strut, which carries load only in compression, can simulate the global seismic response of the CM walls and is suitable for practical applications. Unfortunately, this kind of model does not identify local effects or low ductility zones.

- By comparing the experimental results and the results of the numerical pushover analyses, it was concluded that the strength and stiffness of the wall in the force-displacement curve models proposed by different authors must be calibrated. The calibrated models showed reasonably good agreement with the experimental results. The recommended models should be verified by additional experiments, which will be the subject of future work.

- Good compatibility between the numerical and experimental curves was obtained by the Decanini et al. model, with a slight overestimation in the peak strength of 12%. On the other hand, the best alignment with the experimental results was obtained by the force-displacement curve model proposed by Liberatore et al. with a practically negligible overestimation of the ultimate strength (less than 5%). The reference points of the model were estimated using regression analyses in which the presence of holes in the units, the type of test (monotonic or cyclic), and the type of masonry material were taken into account. None of the remaining four models makes such considerations.

- The considered modern confined masonry appears to have a very good seismic response and a large capacity for energy dissipation.

6. Acknowledgements

7. References

[1] Ghaisas, V.K., Basu, D., Brzev, S., Pérez Gavilán, J.J. (2017): Strut-and-Tie Model for seismic design of confined masonry buildings. *Construction and Building Materials*, **147**, 677–700, doi: https://doi.org/10.1016/j.conbuildmat.2017.04.200

[2] Brzev, S., Hart, T. (2017): Confined masonry network: an overview of guidelines and initiatives, *Proceedings of the 16th World Conference on Earthquake Engineering 16WCEE*, 09-13 January, Santiago, Chile.

[3] Astroza, M., Moroni, O., Brzev, S., Tanner, J. (2012): Seismic Performance of Engineered Masonry Buildings in the 2010 Maule Earthquake. *Special Issue on the 2010 Chile Earthquake. Earthquake Spectra*, **28** (S1), S385-S406.

[4] Miranda, E., Brzev, S., Bijelić, N., Arbanas, Ž., Bartolac, M., Jagodnik, V., Lazarević, D. et al. (2021): StEER-EERI: Petrinja, Croatia December 29, 2020, Mw 6.4 Earthquake Joint Reconnaissance Report (JRR). The Structural Extreme Events Reconnaissance (StEER) Network, United States.

[5] Lang, A.F., Crisafulli, F.J., Torrisi, G.S. (2014): Overview and assessment of analysis techniques for confined masonry buildings, *Proceedings of the 10th National Conference in Earthquake Engineering*, 21-25 July, Anchorage, Alaska.

[6] Singhal, V., Rai, D.C. (2016): In-plane and out-of-plane behavior of confined masonry walls for various toothing and openings details and prediction of their strength and stiffness. *Earthq. Eng. Struct. Dyn*, **45** (15): 2551-2569, doi: https://doi.org/10.1002/eqe.2783

[7] Pérez-Gavilán, J.J., Flores, L.E., Alcocer, S.M. (2015): An experimental study of confined masonry walls with varying aspect ratios. *Earthquake Spectra*, **31** (2): 945–968, doi: https://doi.org/10.1193/090712EQS284M

[8] Marques, R., Pereira, J.M., Lourenço, P.B. (2020): Lateral in-plane seismic response of confined masonry walls: from numerical to backbone models. *Engineering Structures*, **221**, 111098. doi: https://doi.org/10.1016/j.engstruct.2020.111098

[9] Nguyen, L. (2014): Confined Masonry: Theoretical Fundamentals, Experimental Test, Finite Element Models, and Future Uses, PhD Thesis, University of Colorado, Boulder, USA.

[10] Rankawat, N., Brzev, S., Jain, S.K., Pérez Gavilán, J.J. (2021): Nonlinear seismic evaluation of confined masonry structures using equivalent truss model. *Engineering Structures*, **248**, 113114, doi: https://doi.org/10.1016/j.engstruct.2021.113114

[11] Crisafulli, F.J. (1997): Seismic behaviour of reinforced concrete structures with masonry infills, PhD Thesis, University of Canterbury, Christchurch, New Zealand.

[12] Panagiotakos, T.B., Fardis, M.N. (1994): Proposed Nonlinear Strut Models for Infill Panels, 1st year Progress Report of HCM-PREC8 Project, University of Patras.

[13] Decanini, L., Mollaioli, F., Mura, A., Saragoni, R. (2004): Seismic performance of masonry infilled R/C frames, *Proceedings of the 13th World Conference on Earthquake Engineering 13WCEE*, 01-06 August, Vancouver, B.C., Canada.

[14] Dolšek, M., Fajfar, P. (2008): The effect of masonry infills on the seismic response of a four-storey reinforced concrete frame-a deterministic assessment. *Engineering Structures*, **30** (7), 1991-2001, doi: https://doi.org/10.1016/j.engstruct.2008.01.001

[15] Teni, M., Grubišić, M., Guljaš, I. (2014): Simplified Approaches for Modeling Infilled Frames. Electronic *Journal of the Faculty of Civil Engineering Osijek, e-GFOS*, **5** (9), 70-88, doi: http://dx.doi.org/10.13167/2014.9.8

[16] Liberatore, L., Noto, F., Mollaioli, F., Franchin, P. (2018): In-plane response of masonry infill walls: Comprehensive experimentally-based equivalent strut model for deterministic and probabilistic analysis. *Engineering Structures*, **167**, 533-548, doi: https://doi.org/10.1016/j.engstruct.2018.04.057

[17] Saneinejad, A., Hobbs B. (1995): Inelastic design of infilled frames. *Journal of structural engineering*, **121** (4), 634-650, doi: 10.1061/(ASCE)0733-9445(1995)121:4(634)

[18] Žarnić, R., Gostič, S. (1997): Masonry infilled frames as an effective structural sub-assemblage. In: Fajfar, Krawinkler, editors. Seismic Design Methodologies for the Next Generation of Codes. Rotterdam: Balkema, pp. 335-46.

[19] Computers & Structures, Inc. (2016): CSI Analysis Reference Manual for SAP2000, ETABS, SAFE and CSIBridge, Berkeley, California, USA.

[20] Mander, J. B., Priestley, M. J., Park, R. (1988): Theoretical stress-strain model for confined concrete. *Journal of structural engineering*, **114** (8), 1804-1826.